Adiabatic connection in density-functional theory: Two electrons on the surface of a sphere

Michael Seidl
Institute of Theoretical Physics, University of Regensburg, D-93040 Regensburg, Germany
(Received 31 March 2007; published 13 June 2007)

Two interacting electrons that are confined to the surface of a sphere have a uniform ground-state (surface) density. The Schrödinger equation of this helium-type two-electron system is solved here accurately for different values $\alpha \in \mathbb{R}$ of a constant that is multiplied to the electron-electron repulsion $\hat{V}_{ee}$. The correlation structure in the resulting wave functions is analyzed for different values of α. The asymptotic limits $\alpha \to 0$ and $\alpha \to \pm\infty$ are treated analytically. Using these results, the ISI (interaction-strength interpolation) model for the density-functional $E_{xc}[\rho]$ of the exchange-correlation energy in the real system with $\alpha=1$ is tested against the exact adiabatic connection in density-functional theory.

DOI: 10.1103/PhysRevA.75.062506 PACS number(s): 31.15.Ew

I. INTRODUCTION

In recent years, density-functional theory (DFT) [1] has become one of the most frequently applied methods in many-body theory. The basic variable in DFT is not the complicated (correlated) N-particle wave function Ψ, but the simple, non-negative particle density ρ, normalized according to $\int d^3r\, \rho(\mathbf{r})=N$. Each *interacting* N-electron system can be related unambiguously to a fictitious system with the same ground-state density ρ, but with *noninteracting* electrons. The exact ground-state energy of the original (interacting) N-electron system is obtained by solving the Kohn-Sham (KS) single-particle equations of the noninteracting one. In contrast to the Hartree-Fock (HF) equations, the KS equations yield the exact ground-state energy, including the correlation energy which is missed in HF theory (and defined there in a somewhat different way). The only tool that must be approximated in practice is the density functional $E_{xc}[\rho]$ of the exchange-correlation energy.

An exact representation for $E_{xc}[\rho]$ is the coupling-constant integral [2],

$$E_{xc}[\rho] = \int_0^1 d\alpha\, W_\alpha[\rho], \tag{1}$$

where the integrand is defined as a difference,

$$W_\alpha[\rho] \equiv \langle \Psi_\alpha[\rho] | \hat{V}_{ee} | \Psi_\alpha[\rho] \rangle - U[\rho]. \tag{2}$$

Here, $\hat{V}_{ee}$ is the operator of the Coulomb repulsion between the N true *discrete* electrons,

$$\hat{V}_{ee} = \frac{e^2}{2} \sum_{i=1}^{N} \sum_{j(\neq i)=1}^{N} \frac{1}{|\hat{\mathbf{r}}_i - \hat{\mathbf{r}}_j|}, \tag{3}$$

while, overestimating the correct expectation $\langle \hat{V}_{ee} \rangle$, the Hartree functional $U[\rho]$ represents the classical Coulomb energy of a *continuous* charge distribution with density $\rho(\mathbf{r})$,

$$U[\rho] \equiv \frac{e^2}{2} \int d^3r \int d^3r' \frac{\rho(\mathbf{r})\rho(\mathbf{r}')}{|\mathbf{r}-\mathbf{r}'|}. \tag{4}$$

Out of all antisymmetric N-electron wave functions Ψ that are associated with the same given density $\rho=\rho(\mathbf{r})$, $\Psi_\alpha[\rho]$ in Eq. (2) is one that minimizes the expectation $\langle \hat{T}+\alpha\hat{V}_{ee} \rangle$,

$$\langle \Psi_\alpha[\rho] | \hat{T} + \alpha \hat{V}_{ee} | \Psi_\alpha[\rho] \rangle = \min_{\Psi \to \rho} \langle \Psi | \hat{T} + \alpha \hat{V}_{ee} | \Psi \rangle. \tag{5}$$

While $\hat{T}=-(\hbar^2/2m)\Sigma_{i=1}^N \nabla_i^2$ is the usual kinetic-energy operator, the electron-electron repulsion $\hat{V}_{ee}$ is multiplied here with a constant $\alpha \geqslant 0$. Apart from some exceptional cases, $\Psi_\alpha[\rho]$ is usually fixed unambiguously by ρ and an α-dependent external potential $v_{\text{ext}}^\alpha([\rho];\hat{\mathbf{r}})$ exists such that $\Psi_\alpha[\rho]$ is the ground state of the generalized Hamiltonian

$$\hat{H}_\alpha[\rho] = \hat{T} + \alpha \hat{V}_{ee} + \sum_{i=1}^{N} v_{\text{ext}}^\alpha([\rho];\hat{\mathbf{r}}_i). \tag{6}$$

Constructing this α-dependent potential $v_{\text{ext}}^\alpha([\rho];\mathbf{r})$ plus the corresponding ground state $\Psi_\alpha[\rho]$ for a given N-electron density $\rho(\mathbf{r})$ is a nontrivial problem [3]. Generally, $v_{\text{ext}}^{\alpha=1}([\rho];\mathbf{r})$ is the given external potential of the real system. For example, $v_{\text{ext}}^{\alpha=1}([\rho];\mathbf{r})=-Ze^2/r$, for an atom with nuclear charge Ze. On the other hand, $v_{\text{ext}}^{\alpha=0}([\rho];\mathbf{r})$ is the KS external potential that forces N *noninteracting* electrons to have a given ground-state density $\rho=\rho(\mathbf{r})$.

Instead of evaluating the integrand $W_\alpha[\rho]$ for all values $0 \leqslant \alpha \leqslant 1$, one could consider its Taylor expansion about $\alpha=0$ which is equivalent to the Görling-Levy (GL) pertubation expansion [4]. Although computationally demanding, however, this Taylor expansion usually has only a finite radius of convergence α_c, with $\alpha_c < 1$ for many systems of interest [5,6].

A rather simple, but nevertheless reasonably accurate alternative is the interaction-strength interpolation (ISI) model of Ref. [5]. Avoiding convergence problems, ISI keeps only the two leading coefficients $W_0[\rho]$ and $W_0'[\rho]$ of the GL (or weak-interaction) expansion

$$W_\alpha[\rho] = W_0[\rho] + W_0'[\rho]\alpha + \frac{1}{2}W_0''[\rho]\alpha^2 + O(\alpha^3) \quad (\alpha \to 0) \tag{7}$$

and, instead of considering higher-order terms in Eq. (7), makes an extrapolation to the opposite (strong-interaction) limit $\alpha \to \infty$ [7,8],

$$W_\alpha[\rho] = W_\infty[\rho] + \frac{W'_\infty[\rho]}{\sqrt{\alpha}} + \frac{W''_\infty[\rho]}{\alpha} + O(\alpha^{-3/2}) \quad (\alpha \to \infty). \tag{8}$$

[The coefficient of the term $O(\alpha^{-1})$ in expansion (8) is exactly zero, $W''_\infty[\rho] \equiv 0$; see the erratum to Ref. [10] and Sec. IV B below; the primes do not denote derivatives here.] The four leading coefficients $W_0[\rho] \equiv E_x[\rho]$, $W'_0[\rho] \equiv 2E_c^{\mathrm{GL2}}[\rho]$, $W_\infty[\rho]$, and $W'_\infty[\rho]$ of expansions (7) and (8) can be evaluated exactly or accurately for a given density $\rho = \rho(\mathbf{r})$. $E_x[\rho]$ is the DFT exchange energy, and $E_c^{\mathrm{GL2}}[\rho]$ is the second-order correlation energy in the GL pertubation expansion; accurate approximations to the strong-interaction functionals $W_\infty[\rho]$ and $W'_\infty[\rho]$ are presented in Ref. [10]; see also Ref. [7]. For spherical N-electron densities, the probably exact functional $W_\infty[\rho]$ is presented in Ref. [9].

In terms of $x = -2W'_0[\rho]$, $y = W'_\infty[\rho]$, and $z = W_0[\rho] - W_\infty[\rho]$, we define the functionals [5]

$$X[\rho] = \frac{xy^2}{z^2}, \quad Y[\rho] = \frac{x^2y^2}{z^4}, \quad Z[\rho] = \frac{xy^2}{z^3} - 1. \tag{9}$$

Then the ISI model for $W_\alpha[\rho]$ is given by the simple analytical function [5]

$$W_\alpha^{\mathrm{ISI}}[\rho] = W_\infty[\rho] + \frac{X[\rho]}{\sqrt{1 + Y[\rho]\alpha} + Z[\rho]}. \tag{10}$$

By construction, $W_\alpha^{\mathrm{ISI}}[\rho]$ reproduces the two leading terms in each of the two expansions (7) and (8). Although $W_\alpha^{\mathrm{ISI}}[\rho]$ is a smooth and monotonic function of α, its Taylor expansion (7) has a finite radius of convergence. This property is also expected for the unknown true integrand $W_\alpha[\rho]$. Moreover, $W_\alpha^{\mathrm{ISI}}[\rho]$ shares with $W_\alpha[\rho]$ the correct scaling behavior [5,7],

$$W_\alpha[\rho_\lambda] = \lambda W_{\alpha/\lambda}[\rho], \tag{11}$$

where $\rho_\lambda(\mathbf{r}) = \lambda^3 \rho(\lambda \mathbf{r})$ is a scaled density.

Analytical integration of the function (10) yields [5] the ISI model $E_{xc}^{\mathrm{ISI}}[\rho]$ for the exchange-correlation functional (1). It has been applied successfully to atoms, molecules, and the two-dimensional (2D) uniform electron gas [5,10,11]. (Even in the case of the 3D gas where $x = \infty$, ISI does not break down, but becomes only less accurate [10].) In particular, it has turned out that, in contrast to many standard functionals, the ISI correlation energy $E_c^{\mathrm{ISI}}[\rho] = E_{xc}^{\mathrm{ISI}}[\rho] - E_x[\rho]$ is compatible with the exact functional $E_x[\rho]$ for the exchange energy. This property is substantial for a functional to predict the properties of molecules realistically. For any given electron system, only four simple input data are needed: The two leading coefficients in both the weak- and the strong-interaction expansions, Eqs. (7) and (8), of its unknown exact integrand $W_\alpha[\rho]$.

In order to test and improve the accuracy of the model integrand (10), nontrivial electron systems are required where the true integrand $W_\alpha[\rho]$ can be evaluated excatly or accurately. Part of the problem is that, for a given density ρ, the α-dependent external potential $v_{\mathrm{ext}}^\alpha([\rho];\mathbf{r})$ in the Hamiltonian (6) is usually hard to construct. In the present work, however, a two-electron system is investigated where $v_{\mathrm{ext}}^\alpha([\rho];\mathbf{r})$ is known from the beginning.

Section II introduces the Hamiltonian for N electrons that are confined to the surface of a sphere. In Sec. III, the Schrödinger Equation of this system for $N=2$ is simplified to a one-dimensional eigenvalue equation which is easily solved numerically with high accuracy. The resulting numerical wave functions are discussed. The leading coefficients of the expansions (7) and (8) are obtained analytically. These results are used in Sec. IV to evaluate the coupling-constant integrand $W_\alpha[\rho]$ of this system and to compare it to the corresponding ISI model (10) whose coefficients are known analytically here. Results and conclusions are summarized in Sec. V.

II. ELECTRONS CONFINED TO THE SURFACE OF A SPHERE

To find a density $\rho(\mathbf{r})$ for which the external potential $v_{\mathrm{ext}}^\alpha([\rho];\mathbf{r})$ in the Hamiltonian (6) is known for all $\alpha \geqslant 0$, we consider N electrons confined to the 2D surface of a sphere with radius R. (For example, real electrons can be bound on the surface of a droplet of liquid helium.) This situation is described by the limit $\Delta R \to 0$ of the 3D "spherical-shell" potential

$$v_{\mathrm{ext}}(R;\mathbf{r}) = \left\{ \begin{array}{ll} 0: & |r-R| < \frac{1}{2}\Delta R \\ \infty: & \text{elsewhere} \end{array} \right\} \quad (\Delta R \to 0). \tag{12}$$

As $\Delta R \to 0$, the ground-state density becomes

$$\rho_\alpha^{\mathrm{3D}}(\mathbf{r}) = \frac{\delta(r-R)}{R^2} \rho_\alpha(\Omega), \tag{13}$$

where $(r,\Omega) = (r,\theta,\phi)$ are spherical coordinates. Since the potential (12) is isotropic, the 2D (angular) density $\rho_\alpha(\Omega)$ should be uniform, $\rho_\alpha(\Omega) = \frac{N}{4\pi}$, at least for suitable values of the electron number N. [See, however, Eq. (23) below.] Then, the potential $v_{\mathrm{ext}}^\alpha([\rho];\mathbf{r})$ of the Hamiltonian (6) is trivial and given by Eq. (12) for all α. Ignoring the radial degree of freedom, we switch to a strictly 2D description. Then, the wave function only depends on the angular coordinates $\Omega_i \equiv (\theta_i, \phi_i)$ and spin variables σ_i of the electrons $(i = 1 \ldots N)$. The Hamiltonian (6) assumes a 2D form with a constant external potential (which we set to zero),

$$\hat{H}_\alpha^N[R] = -\frac{\hbar^2}{2m_e R^2} \sum_{i=1}^N \Lambda_i + \alpha \sum_{i<j} V_{ee}(\gamma_{ij}),$$

$$\Lambda_i \equiv \frac{1}{\sin\theta_i} \frac{\partial}{\partial \theta_i} \sin\theta_i \frac{\partial}{\partial \theta_i} + \frac{1}{\sin^2\theta_i} \frac{\partial^2}{\partial \phi_i^2}. \tag{14}$$

(Since, in the limit $\Delta R \to 0$, the present system is sufficiently specified by the spherical radius R and the particle number N, we replace from now the symbol "$[\rho]$" by "$[R]$" plus a superscript "N.") The interaction energy $V_{ee}(\gamma_{ij})$ between two electrons depends only on the angle γ_{ij} between their 3D position vectors $\mathbf{r}_i$ and $\mathbf{r}_j$,

$$\cos\gamma_{ij} \equiv \frac{\mathbf{r}_i \cdot \mathbf{r}_j}{R^2} = \cos\theta_i \cos\theta_j + \sin\theta_i \sin\theta_j \cos(\phi_i - \phi_j). \tag{15}$$

For the true 3D Coulomb interaction, we have $V_{ee}(\gamma_{ij}) = e^2|\mathbf{r}_i - \mathbf{r}_j|^{-1}$ or, explicitly,

$$V_{ee}(\gamma) = \frac{e^2}{R\sqrt{2(1-\cos\gamma)}} \equiv \frac{e^2}{R} v(\gamma). \tag{16}$$

Using a properly modified interaction (replacing the "chord distance" $|\mathbf{r}_i - \mathbf{r}_j|$ by the curved distance $R\gamma_{ij}$ along the surface), this system represents for large $N \gg 1$ a *finite* version of the uniform 2D electron gas [12] with no boundary (but in a curved 2D space).

For now, we restrict ourselves to the simplest nontrivial case with $N=2$ electrons (which may be viewed as a poor model for the helium atom). Dropping the superscript $N(=2)$, we write in Eq. (14) $\hat{H}_\alpha[R] = (\hbar^2/m_e R^2)\hat{\mathcal{H}}_{\bar{\alpha}}$, with the dimensionless Hamiltonian

$$\hat{\mathcal{H}}_{\bar{\alpha}} \equiv -\frac{1}{2}(\Lambda_1 + \Lambda_2) + \bar{\alpha} v(\gamma_{12}), \quad \bar{\alpha} \equiv \frac{R\alpha}{a_B}. \tag{17}$$

Here, $a_B = \hbar^2/m_e e^2$ denotes the Bohr radius. The Hamiltonian $\hat{\mathcal{H}}_{\bar{\alpha}}$ has only one independent parameter $\bar{\alpha}$. Obviously, the limit $\alpha \to \infty$ ($\alpha \to 0$) of strong (weak) repulsion is equivalent to the limit $R \to \infty$ ($R \to 0$) of low (high) density. The lowest eigenvalue $\mathcal{E}_\alpha$ of $\hat{\mathcal{H}}_\alpha$ represents the ground-state energy $E_\alpha[a_B]$ of $\hat{H}_\alpha[a_B]$ in units of $e^2/a_B = 1$ hartree. Generally,

$$E_\alpha[R] = \frac{\hbar^2}{m_e R^2}\mathcal{E}_{(\alpha R/a_B)} \equiv \frac{e^2 a_B}{R^2}\mathcal{E}_{(\alpha R/a_B)}. \tag{18}$$

Since $\hat{\mathcal{H}}_\alpha$ does not act on spin variables, we may distinguish a spin-singlet system (S) from an independent spin-triplet system (T) with ground-state energies $\mathcal{E}_\alpha^S$ and $\mathcal{E}_\alpha^T$, respectively. (In spite of our 2D formalism, spin quantization shall be with respect to the real z axis in 3D.)

III. WAVE FUNCTIONS AND DENSITIES

A. Noninteracting case

In the noninteracting case $\alpha=0$, the spatial factor of a singlet eigenfunction of $\hat{\mathcal{H}}_\alpha$ is a symmetrized product (while for a triplet function it is an antisymmetrized product) of two spherical harmonics $Y_{\ell' m'}(\Omega_1)$, $Y_{\ell'' m''}(\Omega_2)$. (The latter are the eigenfunctions of Λ_1 and Λ_2 and play here the role of the single-particle or Kohn-Sham orbitals.) The corresponding eigenvalues of $\hat{\mathcal{H}}_0$ are $\frac{1}{2}[\ell'(\ell'+1) + \ell''(\ell''+1)]$ where $\ell', \ell'' = 0, 1, 2, 3, \ldots$. Consequently, due to the Pauli principle, the lowest singlet (S) and triplet (T) energies for $\alpha=0$ are, respectively,

$$\mathcal{E}_0^S = 0 (\ell' = \ell'' = 0), \quad \mathcal{E}_0^T = 1 (\ell' = 0, \ell'' = 1). \tag{19}$$

The corresponding ground-state spatial wave functions,

$$\Phi_0^S(\Omega_1, \Omega_2) = Y_{00}(\Omega_1) Y_{00}(\Omega_2) \equiv \frac{1}{4\pi}, \tag{20}$$

$$\Phi_0^T(\Omega_1, \Omega_2) = \frac{Y_1(\Omega_1)Y_{00}(\Omega_2) - Y_1(\Omega_2)Y_{00}(\Omega_1)}{\sqrt{2}} \equiv \frac{1}{\sqrt{8\pi}}[Y_1(\Omega_1) - Y_1(\Omega_2)], \tag{21}$$

represent the state $\Psi_{\alpha=0}[\rho]$ in Eq. (2) for the present systems, provided that the resulting ground-state densities will not change when α is set $\neq 0$. In Eq. (21), $Y_1(\Omega)$ may be any normalized linear combination of the $Y_{1m}(\Omega)$ ($m = 0, \pm 1$),

$$Y_1(\Omega) = \sum_{m=0,\pm 1} \eta_m Y_{1m}(\Omega), \tag{22}$$

where $\Sigma_m |\eta_m|^2 = 1$. In other words, ignoring the spin degeneracy, the triplet ground state is threefold degenerate.

While the singlet state (20) has a uniform density, $\rho_0^S(\Omega) \equiv \frac{2}{4\pi}$, the triplet state has not,

$$\rho_0^T(\Omega) = \int d\Omega_2 |\Phi_0^T(\Omega, \Omega_2)|^2 = |Y_{00}|^2 + |Y_1(\Omega)|^2. \tag{23}$$

Obviously, there is no choice for the η_m in Eq. (22) that would make the density (23) uniform. This situation is similar to a (3D) Li atom (with the electron-electron repulsion turned off), held at full spin polarization ($\uparrow\uparrow\uparrow$): In its lowest-energy state, the three electrons must have a nonspherical configuration $1s^1 2s^1 2p^1$ or $1s^1 2p^2$. In the present 2D system, apart from the trivial case $N=1$, at least $N=4$ noninteracting electrons are required for a uniform (spherically symmetric) density in the lowest-energy state with full spin polarization.

B. General case with interacting electrons

Turning to the interacting case $\alpha \neq 0$ of the Hamiltonian (17), we multiply the noninteracting wave functions of the preceding subsection with a Jastrow-type correlation factor $\psi_\alpha^{S,T}(\gamma)$,

$$\Psi_\alpha^{S,T}(\Omega_1, \Omega_2) = \psi_\alpha^{S,T}(\gamma) \Phi_0^{S,T}(\Omega_1, \Omega_2). \tag{24}$$

Here, $\gamma \equiv \gamma_{12}$ is the angle between Ω_1 and Ω_2, given by Eq. (15). For $\alpha=0$, we have $\psi_0^{S,T}(\gamma) \equiv 1$ and $\Psi_0^{S,T} \equiv \Phi_0^{S,T}$ are the Slater determinants of Sec. III A. For $\alpha \neq 0$, in contrast, $\Psi_\alpha^{S,T}$ is a much more complicated (correlated) wave function. The ansatz (24) preserves the correct symmetry of the wave function $\Phi_0^{S,T}$, since γ is invariant upon interchanging Ω_1 and Ω_2.

In the Schrödinger equation $\hat{\mathcal{H}}_\alpha \Psi_\alpha^{S,T} = \mathcal{E}_\alpha^{S,T} \Psi_\alpha^{S,T}$ with the Hamiltonian (17), the ansatz (24) yields eigenvalue equations for $\psi(\gamma)$ (we omit the indices "α" and "S,T" for brevity),

$$S: \quad \psi''(\gamma) = -\frac{\psi'(\gamma)}{\tan\gamma} + [\alpha v(\gamma) - \mathcal{E}_\alpha^S]\psi(\gamma), \tag{25}$$

$$T: \quad \psi''(\gamma) = -2\frac{\psi'(\gamma)}{\tan\gamma} - \frac{\psi'(\gamma)}{\sin\gamma} + [\alpha v(\gamma) + 1 - \mathcal{E}_\alpha^T]\psi(\gamma). \tag{26}$$

For any solution $\psi(\gamma)$ of these equations, the ansatz (24) is an exact eigenfunction of $\hat{\mathcal{H}}_\alpha$. Note that the arbitrary coeffi-

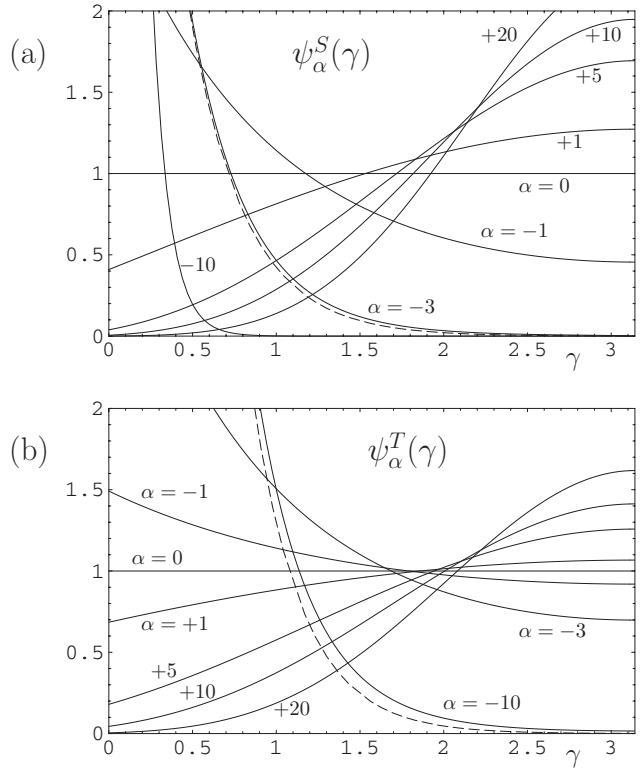

FIG. 1. The normalized correlation factors $\psi_\alpha^{S,T}(\gamma)$ for various values of the parameter α, obtained by numerical solution of Eqs. (25) and (26). The functions (32) (for $\alpha=-3$, S) and (33) (for $\alpha=-10$, T) are shown as dashed curves.

cients η_m in the linear combination (22) do not enter Eq. (26). Consequently, although different choices (22) generate different triplet densities, the triplet correlation factor $\psi_\alpha^T(\gamma)$ and energy $\mathcal{E}_\alpha^T$ are not affected.

The numerical solution of Eqs. (25) and (26) is discussed in Appendix A. It is instructive to study in addition to the realistic situation $\alpha>0$ with repulsive electrons also the situation $\alpha<0$ when the electrons become *attracting* each other. For selected values of α, the resulting normalized functions $\psi(\gamma)$ are plotted in Fig. 1. In the case $\alpha>0$ (repulsive electrons), these functions are increasing monotonically with the angle γ (which is a measure for the distance between the electrons). Consistently, the opposite is true for $\alpha<0$ when the electrons are attracting each other. The numerical eigenvalues $\mathcal{E}_\alpha^S$ and $\mathcal{E}_\alpha^T$ are plotted versus α in Fig. 2 (dots).

While the *singlet density* $\rho_\alpha^S(\Omega)\equiv\frac{2}{4\pi}$ is uniform and independent of α, the *triplet density* $\rho_\alpha^T(\Omega)$ is given by Eq. (A11). There, the coefficient $\tilde{c}_\alpha$ can be evaluated via Eq. (A8) using the numerical functions $\psi_\alpha^T(\gamma)$ shown in Fig. 1(b). $\tilde{c}_\alpha$ is a decreasing function of α, with $\tilde{c}_{-\infty}=3$, $\tilde{c}_0=1$ and $\tilde{c}_{+\infty}=0$ (Fig. 3). Consequently, the triplet density (A11) is nonuniform and changes continuously between the asymptotic functions $\frac{3}{4\pi}-|Y_1(\Omega)|^2$ and $2|Y_1(\Omega)|^2$ as α grows from $-\infty$ to $+\infty$; see also Eqs. (31) and (34) below. Therefore, the triplet wave function $\Psi_\alpha^T(\Omega_1,\Omega_2)$ does not represent the state $\Psi_\alpha[\rho]$ in Eq. (2) for the triplet system. Curiously for one particular interaction strength, $\alpha\approx-5.3$, we find $\tilde{c}_\alpha=2$, such that $\rho_\alpha^T(\Omega)$ coincidentally becomes uniform.

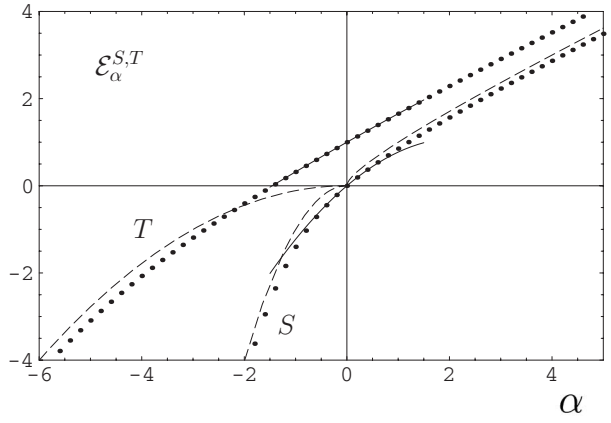

FIG. 2. The singlet (S) and triplet (T) total ground-state energies $\mathcal{E}_\alpha^{S,T}$ for selected values of α (dots). The perturbation expansions (27), truncated at second order, are plotted for $|\alpha|<1.5$ as solid curves. The dashed curves represent the asymptotic strong-repulsion energy (30) ($\alpha>0$) and, respectively, the strong-attraction energies (32) and (33) ($\alpha<0$).

C. Exact limits

Before we address the coupling-constant integrand $W_\alpha[\rho]$ and its ISI model in Sec. IV, we first consider the situation with $|\alpha|\ll1$ (weak interaction), as well as the extreme limits $\alpha\to\infty$ (strong repulsion) and $\alpha\to-\infty$ (strong attraction).

1. Weak interaction

For small $|\alpha|$, $\mathcal{E}_\alpha^S$ and $\mathcal{E}_\alpha^T$ are reproduced by the Møller-Plesset (MP) perturbation expansion [13] for the Hamiltonian $\mathcal{H}_\alpha$ (with respect to α as the small parameter),

$$\mathcal{E}_\alpha^{S,T}=\sum_{n=0}^{\infty}\mathcal{E}_{(n)}^{S,T}\alpha^n \quad (|\alpha|\ll1). \tag{27}$$

At least for the singlet system, the MP expansion is identical with the Görling-Levy (GL) expansion [4], since the density $\rho_\alpha^S(\Omega)$ does not change as the perturbation α is turned on. Consequently, $\mathcal{E}_{(2)}^S$ is the value of the second-order correla-

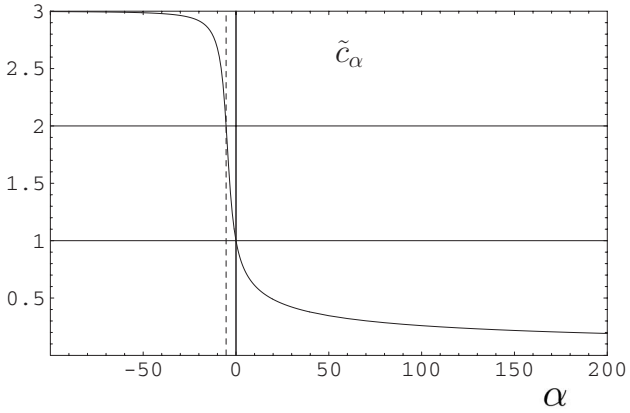

FIG. 3. The coefficient $\tilde{c}_\alpha$ of Eq. (A11) for the triplet density $\rho_\alpha^T(\Omega)$. Only for $\alpha\approx-5.3$ (vertical dashed line), when $\tilde{c}_\alpha=2$, this density is uniform on the sphere.

tion energy $E_c^{GL2}[a_B] \equiv \frac{1}{2} W_0'[a_B]$ in expansion (7) in units of $e^2/a_B = 1$ hartree. Up to second order, the coefficients are known analytically [14],

$$\mathcal{E}^S_{(0)} \equiv \mathcal{E}^S_0 = 0, \quad \mathcal{E}^S_{(1)} = 1,$$

$$\mathcal{E}^S_{(2)} = -(3 - 4\ln 2) = -0.227\,411, \tag{28}$$

$$\mathcal{E}^T_{(0)} \equiv \mathcal{E}^T_0 = 1, \quad \mathcal{E}^T_{(1)} = \frac{2}{3},$$

$$\mathcal{E}^T_{(2)} = -\left(\frac{17}{27} - \frac{8}{9}\ln 2\right) = -0.013\,499. \tag{29}$$

The corresponding second-order truncated expansions are shown in Fig. 2 as solid parabolas.

The radius of convergence, α_c, of the expansion (27) about $\alpha = 0$ is probably finite [5]. In the extreme limits $|\alpha| \to \infty$, on the other hand, Eqs. (25) and (26) are easily solved analytically as we shall see below. Independently, these limits are interpreted physically in Appendixes B and C by simple models.

2. Strong repulsion

For $\alpha \gg 1$, the electrons repel each other strongly. As $\alpha \to +\infty$, they become *strictly correlated* [8]. This phrase refers to a quantum state where the two electrons, upon simultaneous measurement of their positions, are always found exactly opposite to each other on the sphere (Appendix B). This is consistent with Fig. 1 where the correlation factor $\psi^{S,T}_\alpha(\gamma)$ has an increasingly dominant maximum at $\gamma = \pi$ as $\alpha > 0$ grows. Consequently, in this limit, we can put in Eqs. (25) and (26) $\sin\gamma \approx \pi - \gamma \equiv \xi$, $\tan\gamma \approx -\xi$ and expand $v(\gamma) \approx \frac{1}{2} + \frac{1}{16}\xi^2$. The resulting two equations are identical and have the normalized solutions (with normalization factors $\mathcal{N}^{S,T}_\alpha$)

$$\psi^{S,T}_\alpha(\gamma) \to g^{S,T}_\alpha(\gamma) \equiv \mathcal{N}^{S,T}_\alpha e^{-b(\pi-\gamma)^2}, \quad b = \frac{1}{8}\sqrt{\alpha},$$

$$\mathcal{E}^{S,T}_\alpha \to \frac{1}{2}[\alpha + \sqrt{\alpha}] \quad (\alpha \to +\infty). \tag{30}$$

Consequently, for $\alpha \gg 1$, the lower limit 0 of the integrals (A8) may be replaced by $-\infty$. Evaluating the moments (A8) for $\ell \leqslant 2$ to leading order in $\alpha \gg 1$ yields the asymptotic normalization factors $\mathcal{N}^S_\alpha = \alpha^{1/4}$ and $\mathcal{N}^T_\alpha = \frac{1}{2}(4\alpha)^{1/4}$. In particular, we find $\tilde{c}_\infty = 0$, such that the triplet density (A11) becomes

$$\rho^T_\infty(\Omega) \equiv \lim_{\alpha\to\infty} \rho^T_\alpha(\Omega) = 2|Y_1(\Omega)|^2. \tag{31}$$

Confirming the idea of strictly correlated electrons (SCE [8], see Appendix B), the asymptotic behavior (30) of $\mathcal{E}^{S,T}_\alpha$ is identical with the result (B7) for $R = 1$. It is approached very slowly in Fig. 2 (dashed curve for $\alpha > 0$).

3. Strong attraction

In the opposite limit $\alpha \to -\infty$, in contrast, two strongly *attractive* electrons are forming a tightly bound pair (like electron and positron in a 2D positronium atom) that is moving on the sphere as a compact object with approximate radius $\frac{a_B}{|\alpha|} \ll R$. Consequently, the correlation factor $\psi(\gamma)$ is strongly peaked at $\gamma = 0$ in this limit (see Fig. 1). Now, we may put $\tan\gamma$, $\sin\gamma \approx \gamma$ and $v(\gamma) \approx 1/\gamma$ in Eqs. (25) and (26), and the solutions (with normalization factors $\mathcal{M}^{S,T}_\alpha$) become

$$\psi^S_\alpha(\gamma) \to h^S_\alpha(\gamma) \equiv \mathcal{M}^S_\alpha e^{-|\alpha|\gamma},$$

$$\mathcal{E}^S_\alpha \to -\alpha^2 \quad (\alpha \to -\infty), \tag{32}$$

$$\psi^T_\alpha(\gamma) \to h^T_\alpha(\gamma) \equiv \mathcal{M}^T_\alpha e^{-|\alpha|\gamma/3},$$

$$\mathcal{E}^T_\alpha \to -\frac{1}{9}\alpha^2 \quad (\alpha \to -\infty). \tag{33}$$

The normalization conditions $c^S_{\alpha,0} = 1$ and $c^T_{\alpha,0} - \frac{1}{3}c^T_{\alpha,1} = 1$, with Eq. (A8) for $c^{S,T}_{\alpha,\ell}$, imply $\mathcal{M}^S_\alpha = 2^{3/2}|\alpha|$ and $\mathcal{M}^T_\alpha = (\frac{2}{3})^{5/2}\alpha^2$ as $\alpha \to -\infty$ [when the upper limit π of the integrals (A8) may be replaced by ∞]. The asymptotic functions $h^{S,T}_\alpha(\gamma)$ are shown in Fig. 1 as dashed curves for $\alpha = -3$ (S) and for $\alpha = -10$ (T). The asymptotic energies $-\alpha^2$ and $-\frac{1}{9}\alpha^2$ are shown as dashed curves for $\alpha < 0$ in Fig. 2. Confirming the idea of a compact attractive-electron pair, the energies $\mathcal{E}^{S,T}_\alpha$ for $\alpha \to -\infty$ approach the two lowest eigenvalues E_0 and E_1 of 2D positronium as $\alpha \to -\infty$, Eq. (C7) in Appendix C.

Even the wave functions (C8) of Appendix C can be extracted from the behavior of the present system in the limit $\alpha \to -\infty$ [14]. Integrating the resulting expression yields

$$\rho^T_{-\infty}(\Omega) = \frac{3}{4\pi} - |Y_1(\Omega)|^2, \tag{34}$$

confirming the earlier result $\tilde{c}_{-\infty} = 3$ in Eq. (A11).

IV. CORRELATION ENERGY IN THE SINGLET SYSTEM

The main goal of the present work is to test the ISI model (10) of Ref. [5] for the coupling-constant integrand $W_\alpha[\rho]$ in Eq. (1). Such a test requires an electron system whose ground-state density ρ does not change as the strength α of the electronic repulsion is varied. As we have seen in Sec. III, the present system with two electrons on a sphere just has this property, at least when the electrons are in the singlet state. As in Sec. II, we use for this system the notation $W_\alpha[R]$, $\Psi_\alpha[R]$ for $W_\alpha[\rho]$, $\Psi_\alpha[\rho]$, etc.

A. Coupling-constant integrand

The singlet wave function $\Psi^S_{\bar\alpha}(\Omega_1, \Omega_2) \equiv \frac{1}{4\pi}\psi^S_{\bar\alpha}(\gamma)$, with $\bar\alpha = \alpha R/a_B$, represents the state $\Psi_\alpha[R]$ in Eq. (2) for the coupling-constant integrand of the singlet system,

$$W_\alpha[R] = \frac{e^2}{R}\int d\Omega_1 \int d\Omega_2\, v(\gamma)|\Psi^S_{\bar\alpha}(\Omega_1,\Omega_2)|^2 - U[R]$$

$$\equiv \frac{e^2}{2R}\int_0^\pi d\gamma \sin\gamma v(\gamma)|\psi^S_{\bar\alpha}(\gamma)|^2 - \frac{2e^2}{R}. \tag{35}$$

Here, Eq. (16) was used for $\hat{V}_{ee}$ in Eq. (2), and the Hartree

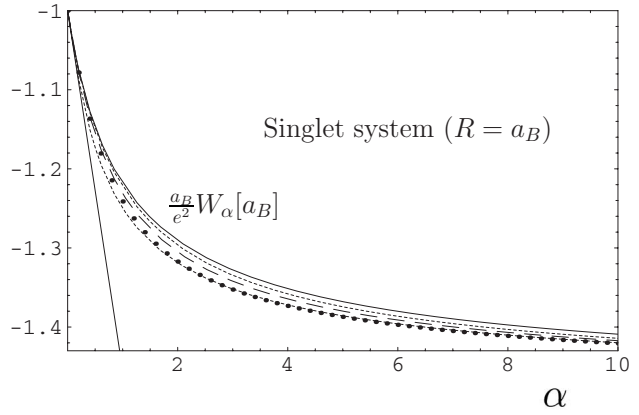

FIG. 4. The accurate numerical coupling-constant integrand $W_\alpha[R]$ (large dots) for the singlet system (with $R=a_B$). The inclined solid straight line represents the first-order Taylor expansion $W_\alpha^{(2)}=W_0+\alpha W_0'$ of $W_\alpha[a_B]$ using the exchange energy $E_x[a_B]=W_0$ and the second-order correlation energy $E_c^{\mathrm{GL2}}[a_B]=\frac{1}{2}W_0'$. Enormous improvement is found in the ISI model (10), shown as a solid curve, using $W_\infty[a_B]=-\frac{3}{2}\frac{e^2}{a_B}$ and the parameters (40). The long-dashed curve represents the ISI3 model (41) with the parameters listed in row (iii) of Table I. The upper and lower short-dashed curves (the latter one almost on top of the dots representing the exact $W_\infty[a_B]$), respectively, correspond to rows (i) and (ii) of Table I.

energy $U[R]=Q^2/2R$ is the electrostatic energy of a uniform continuous surface charge $Q=-2e$ on the sphere. Due to the scaling behavior (11) of the general integrand $W_\alpha[\rho]$ in Eq. (1), the function (35) satisfies the relation

$$W_\alpha[R]=\frac{a_B}{R}W_{(\alpha R/a_B)}[a_B]. \tag{36}$$

This result has a simple graphical interpretation. The plot of $W_\alpha[R]$ vs α is obtained from the one of $W_\alpha[a_B]$ simply by zooming with the factor $\frac{a_B}{R}$. In particular, without loss of generality, we may confine ourselves to the case $R=a_B$. With the numerical correlation factors $\psi_\alpha^S(\gamma)$ described in Sec. III, Eq. (35) yields values for $W_\alpha[a_B]$ which are represented by dots in Fig. 4.

To test the numerical accuracy, first note that $\hat{V}_{ee}\equiv\partial\hat{H}_\alpha[R]/\partial\alpha$, since the Hamiltonian (14) has no α-dependent external potential. Therefore, the Hellmann-Feynman theorem ensures that $\langle\Psi_\alpha^S[R]|\hat{V}_{ee}|\Psi_\alpha^S[R]\rangle=\partial E_\alpha^S[R]/\partial\alpha$, and we have

$$W_\alpha[R]=\frac{\partial E_\alpha^S[R]}{\partial\alpha}-U[R]. \tag{37}$$

Numerical differentiation of $\mathcal{E}_\alpha^S=\frac{a_B}{e^2}E_\alpha^S[a_B]$ yields via Eq. (37) values for $\frac{a_B}{e^2}W_\alpha[a_B]$ that deviate by less than 0.0001 from the corresponding results obtained directly from Eq. (35). Such a small deviation is invisible in Fig. 4. It is completely negligible against the difference from the ISI model $W_\alpha^{\mathrm{ISI}}[a_B]$, solid curve in Fig. 4, which shall be analyzed below. This observation suggests that the present numerical results for $W_\alpha[a_B]$ are very accurate.

TABLE I. Coefficients of the ISI and the ISI3 models for $W_\alpha^S[R]$.

(Singlet)	X	Y	Z	Q	W_0''
ISI	0.227	0.827	−0.545	(∞)	1.016
ISI3 (i)	0.227	0.827	+1.352	0.921	0.964
ISI3 (ii)	0.227	0.827	−0.807	0.328	−0.762
ISI3 (iii)	0.156	0.390	−0.860	0.561	0.710

B. Test of the ISI model

The coefficients of the two leading terms in both Eqs. (7) and (8) are known analytically for the present system. Via Eq. (37), using Eqs. (27), (28), and (30), they can be read off Eq. (18),

$$W_0[R]=-\frac{e^2}{R},\quad W_0'=-2(3-4\ln 2)\frac{e^2}{a_B}, \tag{38}$$

$$W_\infty[R]=-\frac{3}{2}\frac{e^2}{R},\quad W_\infty'[R]=\frac{1}{4}\left(\frac{a_B}{R}\right)^{3/2}\frac{e^2}{a_B}. \tag{39}$$

The ISI model $W_\alpha^{\mathrm{ISI}}[R]$ for $W_\alpha[R]$ is given by Eq. (10), with $W_\infty[R]=-\frac{3}{2}\frac{e^2}{R}$ and

$$X[R]=C\frac{e^2}{R},\quad Y[R]=16C^2\frac{R}{a_B},$$

$$Z=2C-1\quad(C=3-4\ln 2). \tag{40}$$

For $R=a_B$, these parameters are listed in the row "ISI" of Table I. The R dependences in Eqs. (38) and (39) guarantee that $W_\alpha^{\mathrm{ISI}}[R]$ has the correct scaling behavior (36).

From now, we put $R=a_B$ and drop the argument $[a_B]$ for the rest of this subsection. W_α^{ISI} is plotted in Fig. 4 (solid curve), modeling the "exact" W_α (dots) reasonably well. To appreciate the success of this model, note that ISI uses the perturbation (or weak-interaction) expansion only up to the second order. This information alone would predict for W_α the linear function $W_\alpha^{(2)}=W_0+\alpha W_0'$, shown as an inclined solid line in Fig. 4. To transform this extremely poor prediction into the realistic function W_α^{ISI}, only two additional coefficients W_∞ and W_∞' from the simple opposite (strong-interaction) limit $\alpha\to\infty$ are employed.

For large $\alpha\gg 1$, the small ISI error in Fig. 4 is due to the spurious nonzero value $-\frac{XZ}{Y}$, predicted by the ISI function W_α^{ISI} for the coefficient $W_\infty''\equiv 0$ in expansion (8). To estimate the effect of this shortcoming, we re-define the values of X, Y, and Z, and consider the modified function

$$W_\alpha^{\mathrm{ISI3}}=W_\infty+\frac{X}{\sqrt{1+Y\alpha}+Z}+\frac{XZ}{Y(Q+\alpha)}. \tag{41}$$

It has an extra parameter $Q>0$, but no spurious term $O(\alpha^{-1})$ as $\alpha\to\infty$. The new parameter shall be used below to enforce

the correct *second* derivative $W_0'' \equiv (d^2W_\alpha/d\alpha^2)|_{\alpha=0} = 6E_c^{\mathrm{GL3}}$. Then, the first *three* terms (rather than the first two) in both expansions (7) and (8) of the true integrand $W_\alpha[R]$ are reproduced exactly. Therefore, the present model is labeled "ISI3," whereupon the original ISI of Ref. [5] should logically be called "ISI2."

To keep the correct coefficient of the $O(\alpha^{-1/2})$ term, we must set $X = W_\infty' \sqrt{Y}$, as in Eq. (40). Comparing the two leading terms in the expansion of the function (41) about $\alpha = 0$ with Eq. (7) yields two equations for the remaining three parameters Q, Y, and Z,

$$\frac{W_0 - W_\infty}{W_\infty'} = \frac{\sqrt{Y}}{Z+1} + \frac{Z}{Q\sqrt{Y}}, \tag{42}$$

$$\frac{W_0'}{W_\infty'} = \frac{\sqrt{Y^3}}{2(Z+1)^2} + \frac{Z}{Q^2\sqrt{Y}}. \tag{43}$$

Eliminating Q,

$$Q = \frac{Z}{a\sqrt{Y} - \dfrac{Y}{1+Z}}, \quad a \equiv \frac{W_0 - W_\infty}{W_\infty'} > 0, \tag{44}$$

writing $\frac{W_0'}{W_\infty'} \equiv b$, and taking $\sqrt{Y} \equiv c$ for known, we are left with a cubic equation for Z,

$$Z^3 + \left[2 + \frac{a^2 c}{b}\right] Z^2 + \left[1 + \frac{c}{2b}(2a - c)^2\right] Z + \frac{c}{b}(a - c)^2 = 0. \tag{45}$$

Using, rather arbitrarily, for $Y = c^2$ the ISI value Y^{ISI} (by putting $c = -\frac{2b}{a^2}$), the three solutions of Eq. (45) would be $Z_0 = -\left(1 + \frac{2b}{a^3}\right)$ and

$$Z_{1,2} = \frac{1}{2}[-Z_0 \pm \sqrt{Z_0(Z_0 - 8)}]. \tag{46}$$

Solution Z_0 is useless, since it implies $Q = \infty$, recovering in Eq. (41) the original ISI function (10). For the present system where $a = 2$ and $b = -8C$, solution Z_1 yields only slight improvement beyond ISI [upper short-dashed curve in Fig. 4, row (i) in Table I], while solution Z_2 seems to provide an accurate model [lower short-dashed curve in Fig. 4, row (ii) in Table I]. Almost invisible in Fig. 4, however, the second derivative of W_α^{ISI3} at $\alpha = 0$ is *negative* in this case (see the last column in Table I), implying a spurious inflection point at $\alpha \approx 0.033$.

While the choice $Y = Y^{\mathrm{ISI}}$ is quite arbitrary, Y can be chosen in such a way that W_α^{ISI3} has the correct second derivative at $\alpha = 0$, $W_0'' \equiv (d^2W_\alpha/d\alpha^2)|_{\alpha=0} = 6E_c^{\mathrm{GL3}}$. Completing the set of Eqs. (42) and (43), this condition yields the third equation for the three parameters Q, Y, and Z (recall that $X = W_\infty' \sqrt{Y}$),

$$W_0'' = \frac{XY^2}{4} \frac{Z+3}{(Z+1)^3} + \frac{2XZ}{YQ^3}. \tag{47}$$

Equivalently, Eqs. (45) and (47) represent *two* equations for *two* unknowns Z and $Y \equiv c^2$. For the present system, $W_0'' = 6\mathcal{E}_{(3)}^S \frac{e^2}{a_B}$ can be found numerically, $W_0'' \approx 0.71 \frac{e^2}{a_B}$. (Note that W_0'', unlike W_0', is R-dependent and generally given by $W_0''[R] = W_0''[a_B]\frac{R}{a_B} \approx 0.71 \frac{Re^2}{a_B^2}$.) This is positive, but smaller than the ISI prediction $\frac{a_B}{e^2}(d^2W_\alpha^{\mathrm{ISI}}/d\alpha^2)|_{\alpha=0} = 16C^2(C+1) = 1.02$ (last column in Table I). Only for one particular value of Y (or $c = \sqrt{Y}$), Eq. (45) has a solution Z [row (iii) in Table I, long-dashed curve in Fig. 4] that fulfills condition (47) with $W_0'' = 0.71 \frac{e^2}{a_B}$ and at the same time yields in Eq. (44) a positive value for Q. (The other two solutions for the same Y do not.)

Using two additional exact asymptotic parameters, $W_0'' = 0.71 \frac{e^2}{a_B}$ and $W_\infty'' = 0$, ISI3 is more accurate than the original ISI (or ISI2) model. This improvement will be discussed further in the following subsection. For general systems, however, evaluation of $W_0'' = 6E_c^{\mathrm{GL3}}$ is even more expensive than that of E_c^{GL2}. Moreover, it is not guaranteed, that there is always a value c for which Eq. (45) has a solution that fulfills condition (47) and yields $Q > 0$ in Eq. (44). Apart from these limitations and difficulties, the ISI3 integrand (41), sharing all the exact properties, is more accurate than the original ISI model. Just as the ISI integrand (10), the ISI3 integrand (41) can be integrated analytically in Eq. (1). Unlike the ISI coefficients, Eq. (9), however, the ISI3 coefficients Y and Z have no explicit expressions, but are given implicitly as solutions of cubic equations [while $X = W_\infty' \sqrt{Y}$ and Q, Eq. (44), are explicit functions of Y and Z].

C. Singlet correlation energies

Integration $\int_0^1 d\alpha$ in Eq. (37) yields the exchange-correlation energy (1) of the realistic system (with $\alpha = 1$) as a function of R. Since $E_0^S[R] = 0$, see Eq. (28), we obtain

$$E_{xc}^S[R] \equiv \int_0^1 d\alpha\, W_\alpha[R] = E_1^S[R] - U[R] = \frac{e^2 a_B}{R^2} \mathcal{E}_{R/a_B}^S - 2\frac{e^2}{R}, \tag{48}$$

where Eq. (18) has been applied in the second step.

In the high-density limit $R \to 0$, we may use the weak-interaction expansion (27) for $\mathcal{E}_\alpha$ which has no zero-order term, $\mathcal{E}_{(0)}^S = 0$; see Eq. (28). Representing the *exchange energy* $E_x[R] \equiv W_0[R] = -\frac{e^2}{R}$, the first-order term (with $\mathcal{E}_{(1)}^S = 1$) becomes dominant as $R \to 0$. The remaining *correlation energy* $E_c[R] = E_{xc}[R] - E_x[R]$,

$$E_c^S[R] = \frac{e^2 a_B}{R^2} \mathcal{E}_{R/a_B}^S - \frac{e^2}{R}, \tag{49}$$

is for small R dominated by the constant (R-independent) second-order term $E_c^{\mathrm{GL2}} = \frac{e^2}{a_B}\mathcal{E}_{(2)}^S$,

$$E_c^S[R] = \frac{e^2}{a_B}\mathcal{E}_{(2)}^S + \frac{e^2 R}{a_B^2}\mathcal{E}_{(3)}^S + O(R^2) \tag{50}$$

(with $\mathcal{E}_{(2)}^S = -C = -0.227\,411$). For finite densities (with $R \gg a_B$), however, E_c^{GL2} as an approximation to $E_c^S[R]$ becomes extremely poor, see Table II. The "exact" values there are obtained from Eq. (49) using the numerical values $\mathcal{E}_\alpha^S$.

Vast improvement beyond E_c^{GL2} is found in the ISI model (third column in Table II),

TABLE II. Correlation energies $E_c[R]$ of the singlet system in second-order perturbation theory (GL2), in the ISI model (51), and in the ISI3 model, using the function (41) and the additional coefficients $W_0''[a_B] \approx 0.71\frac{e^2}{a_B}$ and $W_\infty'' \equiv 0$. The "exact" values are obtained numerically via Eq. (49).

R	GL2	ISI	ISI3	Exact
0.1	−0.2274	−0.2118	−0.2157	−0.2175
0.2	−0.2274	−0.1985	−0.2045	−0.2064
0.5	−0.2274	−0.1679	−0.1760	−0.1796
1.0	−0.2274	−0.1349	−0.1426	−0.1473
2.0	−0.2274	−0.0984	−0.1040	−0.1081
5.0	−0.2274	−0.0562	−0.0587	−0.0605
10.0	−0.2274	−0.0337	−0.0348	−0.0355

$$E_c^{\mathrm{ISI}}[R] \equiv \int_0^1 d\alpha\, W_\alpha^{\mathrm{ISI}}[R] = \frac{e^2 a_B}{8CR^2}\left[k(R) - (2C-1)\ln\left(1+\frac{k(R)}{2C}\right)\right] - \frac{e^2}{2R}, \tag{51}$$

where $k(R)=\sqrt{1+16C^2R/a_B}-1$. The mean absolute error of the ISI correlation energies in Table II is 0.0076 hartree or 4.8 kcal/mole. By construction, ISI is particularly accurate for $R \ll a_B$ and for $R \gg a_B$. The maximum error occurs at $R \approx a_B$.

The ISI model for the integrand $W_\alpha[R]$ uses only the first two terms, $W_0[R]=E_x[R]$ and $W_0'=2E_c^{\mathrm{GL2}}$, of the weak-interaction (or Taylor) expansion (7) for small $\alpha \ll 1$. Instead of considering higher-order terms, the two parameters $W_\infty[R]$ and $W_\infty'[R]$ from the opposite strong-interaction expansion (8) for $\alpha \gg 1$ are introduced. The success of this "interaction-strength interpolation" is quite remarkable. Note that the Taylor expansion of $W_\alpha[R]$ about $\alpha=0$ is expected to have only a finite radius $\alpha_c[R]$ of convergence. Therefore, even when all orders are considered, $W_\alpha[R]$ can be constructed only for $\alpha \leqslant \alpha_c[R]$. In this sense, ISI is simulating a resummation of the divergent perturbation expansion [5].

As a natural extension of ISI, the ISI3 model (41) uses two additional asymptotic coefficients: The $O(\alpha^2)$ coefficient $W_0''[R] \approx 0.71Re^2/a_B^2$ from the weak-interaction expansion (7) plus the $O(\alpha^{-1})$ coefficient $W_\infty'' \equiv 0$ from the strong-interaction expansion (8). Not surprisingly, the resulting ISI3 correlation energies $E_c^{\mathrm{ISI3}}[R]=\int_0^1 d\alpha\, W_\alpha^{\mathrm{ISI3}}[R]$, using the parameters in row (iii) of Table I, are more accurate (fourth column in Table II) than the ISI values. Their mean absolute error amounts only 0.0027 hartree or 1.7 kcal/mol. Requiring the third-order of the GL perturbation expansion, however, this improvement is bought at a high price.

In concluding, we consider the kinetic-energy contribution $T_c[\rho]$ to the correlation energy. Using the notation $\langle\cdots\rangle_\alpha$ for expectation values in the state $\Psi_\alpha[\rho]$, the generalized correlation energy $E_c^\alpha[\rho]=\int_0^\alpha d\beta\, W_\beta[\rho]-\alpha E_x[\rho]$, with $E_c^{\alpha=1}[\rho]=E_c[\rho]$, can be written as

$$E_c^\alpha[\rho] = (\langle\hat{T}\rangle_\alpha - \langle\hat{T}\rangle_0) + \alpha(\langle\hat{V}_{ee}\rangle_\alpha - \langle\hat{V}_{ee}\rangle_0), \tag{52}$$

where $\langle\hat{T}\rangle_0 \equiv T_s[\rho]$ is the density functional of the noninteracting kinetic energy. The enhancement of kinetic energy due to the interaction $\alpha\hat{V}_{ee}$ in the Hamiltonian (6),

$$T_c^\alpha[\rho] = (\langle\hat{T}\rangle_\alpha - \langle\hat{T}\rangle_0), \tag{53}$$

is an important contribution to $E_c^\alpha[\rho]$. Combining Eqs. (52) and (53), we find

$$T_c^\alpha[\rho] = E_c^\alpha[\rho] - \alpha(W_\alpha[\rho] - W_0[\rho]), \tag{54}$$

where we have used the definition (2) of $W_\alpha[\rho]$. The weak-interaction expansion (7) implies that $E_c^\alpha[\rho]=E_c^{\mathrm{GL2}}[\rho]\alpha^2 + O(\alpha^3)$ (recall that $W_0[\rho]\equiv E_x[\rho]$ and $W_0'[\rho]\equiv 2E_c^{\mathrm{GL2}}[\rho] < 0$) and thus

$$T_c^\alpha[\rho] = |E_c^{\mathrm{GL2}}[\rho]|\alpha^2 + O(\alpha^3) \quad (\alpha \to 0). \tag{55}$$

On the other hand, since $T_c^\alpha[\rho]=\int_0^\alpha d\beta\, W_\beta[\rho]-\alpha W_\alpha[\rho]$, the scaling behavior (11) implies that

$$T_c^\alpha[\rho_\lambda] = \lambda^2 T_c^{(\alpha/\lambda)}[\rho]. \tag{56}$$

In the present (singlet) system, the energy at $\alpha=0$ is purely kinetic. Moreover, since $\mathcal{E}_0^S=0$, see Eq. (19), we have $T_s[R]=0$ such that $T_c^\alpha[R]$ is for all R the *full* kinetic energy in the state $\Psi_\alpha[R]$. Equation (56) implies the scaling behavior $T_c^\alpha[R]=\left(\frac{a_B}{R}\right)^2 T_c^{\bar{\alpha}}[a_B]$, with $\bar{\alpha}=\alpha R/a_B$. Therefore, we may confine ourselves to the case $R=a_B$. Figure 5 shows $T_c^\alpha[a_B]$ for $-1 \leqslant \alpha \leqslant +5$. The quadratic behavior (55) around $\alpha=0$ is evident. For $\alpha \to +\infty$, the virial theorem for the harmonic oscillator, given by the Hamiltonian (B6) in Appendix B, demands that $\frac{a_B}{e^2}T_c^\alpha[a_B] \to \frac{1}{4}\sqrt{\alpha}$. For $\alpha \to -\infty$, in contrast, the virial theorem for the 2D attractive-electron pair in Appendix C implies that $T_c^\alpha[a_B] \to -E_0 = +\alpha^2\frac{e^2}{a_B}$; see Eq. (C7).

V. SUMMARY AND CONCLUSIONS

We have considered here a nontrivial (interacting) two-electron system where the ground-state electron density does not change when the Coulomb repulsion between the electrons is multiplied by an arbitrary real number $\alpha \neq 1$. For such a system, the external potential $v_{\mathrm{ext}}^\alpha([\rho];\hat{\mathbf{r}})$ in the Hamiltonian (6) is known and, trivially, is the same for all $\alpha \in \mathbb{R}$. Consequently, the coupling-constant integrand $W_\alpha[R]$ of this system can be obtained directly by solving a regular Schrödinger equation. Moreover, this Schrödinger equation

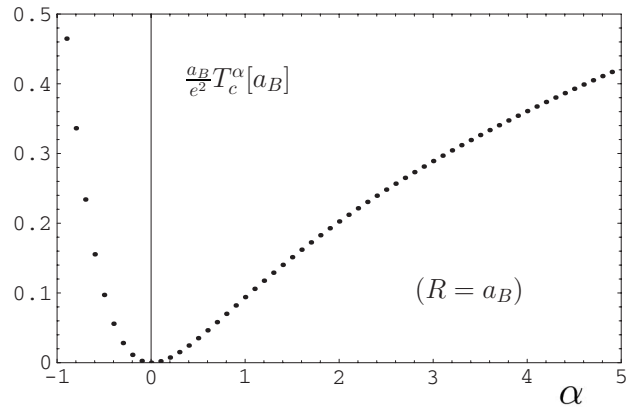

FIG. 5. The enhancement $T_c^\alpha[R]$ of the kinetic energy $T^\alpha[R]$ of the interacting system beyond the noninteracting value $T_s[R]$. In the present case, $T_s[R]=0$, such that $T_c^\alpha[R] \equiv T^\alpha[R]$ is simply the *full* kinetic energy.

can be simplified to a one-dimensional eigenvalue equation. The numerical solution of this simple equation is very accurate, at least when the interaction strength α is not extremely large.

Knowing the exact integrand $W_\alpha[R]$, we are able to test its ISI model $W_\alpha^{\mathrm{ISI}}[R]$ of Ref. [5]. This test is all the more efficient here, since the four ISI coefficients $W_0[R]$, W_0', $W_\infty[R]$, and $W_\infty'[R]$, and then also the ISI model $W_\alpha^{\mathrm{ISI}}[R]$, are known analytically for this system. As can be seen in Fig. 4, $W_\alpha^{\mathrm{ISI}}[R]$ is reasonably accurate. The same is true for the corresponding ISI correlation energies in Table II. This success of the ISI approach is particularly remarkable, since ISI uses only the two leading terms of the perturbation expansion (7). This information alone cannot provide any reasonable prediction for finite values $\alpha \approx 1$, see the inclined straight line in Fig. 4. As the only additional information, however, ISI uses the two leading terms of the strong-interaction limit (8).

The present example for an exact integrand $W_\alpha[R]$ is not only useful for a test of the ISI model, but, in particular, for constructing new functionals for the correlation energy. Using *three* instead of only two leading terms in both the expansions (7) and (8), the extended ISI model of Sec. IV B, called "ISI3" here, improves the ISI results considerably. Since ISI3 requires evaluation of the third order in the perturbation expansion of Ref. [4] (which is known accurately only for the present system), however, this improvement is bought at a high price.

In addition to this analysis of the ISI approach, the correlated two-electron wave functions have been studied and illustrated in Fig. 1 for different values of the interaction strength α. The corresponding ground-state energies are shown in Fig. 2. For this study, also *negative* values of α (describing *attractive* electrons) are included. Particular attention is drawn to the extreme limits $\alpha \to +\infty$ and $\alpha \to -\infty$. These limits are treated analytically in Appendixes B and C, respectively. For both positive and negative values of α, the kinetic energy is enhanced over its noninteracting value at $\alpha=0$, as can be seen in Fig. 5. Curiously, in contrast to the spin-singlet system, the triplet system does *not* have a constant uniform density, but one that changes as the parameter α is varied. The only exception is the accidental case $\alpha \approx -5.3$ when the triplet state has a uniform ground-state density.

APPENDIX A: SOLVING THE SCHRÖDINGER EQUATION

1. Correlation factors $\psi_\alpha^{S,T}(\gamma)$

The function $\psi(\gamma)$ in Eqs. (25) and (26) has the domain $\gamma \in [0,\pi]$. For $|\gamma| \ll 1$ when $v(\gamma) \approx \frac{1}{\gamma}$ and $\tan\gamma \approx \sin\gamma \approx \gamma$, we expand $\psi(\gamma)=\psi(0)+\psi'(0)\gamma+\frac{1}{2}\psi''(0)\gamma^2+\cdots$ to find from Eqs. (25) and (26) the *cusp conditions*

$$S: \quad \psi'(0) = \alpha\psi(0),$$

$$\psi''(0) = \frac{1}{2}[\alpha^2 - \mathcal{E}_\alpha^S]\psi(0), \tag{A1}$$

$$T: \quad \psi'(0) = \frac{1}{3}\alpha\psi(0),$$

$$\psi''(0) = \frac{1}{12}[\alpha^2 - 3(\mathcal{E}_\alpha^T - 1)]\psi(0). \tag{A2}$$

For $\gamma=\pi$, in contrast, when the two electrons are at opposite positions on the sphere, the wave function cannot have a cusp. This implies the *eigenvalue condition*

$$\psi'(\pi) = 0. \tag{A3}$$

For the lowest-energy state, ψ must be node-free, $\psi(\gamma) \neq 0$ for $0 \leqslant \gamma \leqslant \pi$. In this case, the wave function (24) represents the state $\Psi_\alpha[\rho]$ in Eq. (1), at least for the singlet system. According to conditions (A1) and (A2) for $\psi'(0)$, and consistent with intuition, $|\psi(\gamma)|^2$ has for repulsive electrons ($\alpha > 0$) a minimum, but for attractive ones ($\alpha < 0$) a *maximum* at $\gamma=0$.

Starting at $\gamma=0$ with the cusp conditions (A1) and (A2), Eqs. (25) and (26) are easily integrated numerically up to the point $\gamma=\pi$ where the eigenvalue condition (A3) is used for selecting the physical solutions ("eigenfunctions"). The results of such a numerical integration are presented in Fig. 1.

At least for special values of α, even analytical solutions exist [see Eqs. (30), (32), and (33)]. Substituting $\psi(\gamma)=f(\cos\gamma)$ and writing $\cos\gamma=x$, Eqs. (25) and (26) assume a more familiar form,

$$S: \quad (1-x^2)f''(x) - 2xf'(x) + [\mathcal{E}_\alpha^S - \alpha\tilde{v}(x)]f(x) = 0, \tag{A4}$$

$$T: \quad (1-x^2)f''(x) - (3x+1)f'(x) + [\mathcal{E}_\alpha^T - 1 - \alpha\tilde{v}(x)]f(x) = 0, \tag{A5}$$

where $\tilde{v}(x)=[2(1-x)]^{-1/2}$. For $\alpha=0$, Eq. (A4) is Legendre's differential equation. Its solutions are the Legendre polynomials, $f(x)=P_\ell(x)$, with $\mathcal{E}_0^S=\ell(\ell+1)$ and $\ell=0,1,2,\ldots$. For $\ell>0$, these solutions correspond to certain *excited* states $\tilde{\Phi}_0^S$

of the noninteracting system with $\ell' = \ell'' = \ell$. This is evident from the addition theorem for spherical harmonics,

$$\tilde{\Phi}_0^S(\Omega_1,\Omega_2) \propto \frac{P_\ell(\cos\gamma)}{4\pi} \equiv \frac{1}{2\ell+1}\sum_{m=-\ell}^{\ell} Y_{\ell m}^*(\Omega_1) Y_{\ell m}(\Omega_2). \tag{A6}$$

For $\alpha \neq 0$, however, the solutions $f(x)$ of Eq. (A4) cannot be polynomials, since the cusp condition (A1) implies that $|f'(1)| = \infty$. Note, however, that the function $\tilde{v}(x)$ is closely related to the Legendre polynomials, $\tilde{v}(x) \equiv \Sigma_{\ell=0}^{\infty} P_\ell(x)$.

2. Densities $\rho_\alpha^{S,T}(\Omega)$

Eventually, we consider the *electron density* $\rho_\alpha^{S,T}(\Omega)$ in the state (24). For $\alpha = 0$ we have $\psi_0^{S,T}(\gamma) \equiv 1$. For the general case, we expand in terms of the $P_\ell(x)$,

$$|\psi_\alpha^{S,T}(\gamma)|^2 = \sum_{\ell=0}^{\infty} c_{\alpha,\ell}^{S,T} P_\ell(\cos\gamma), \tag{A7}$$

$$c_{\alpha,\ell}^{S,T} = \frac{2\ell+1}{2}\int_0^\pi d\gamma \sin\gamma P_\ell(\cos\gamma)|\psi_\alpha^{S,T}(\gamma)|^2, \tag{A8}$$

where $c_{0,\ell}^{S,T} = \delta_{\ell,0}$. Then, we have

$$\begin{aligned}\rho_\alpha^{S,T}(\Omega_1) &= 2\int d\Omega_2 |\psi_\alpha^{S,T}(\gamma)|^2 |\Phi_0^{S,T}(\Omega_1,\Omega_2)|^2 \\ &= 2\sum_{\ell=0}^{\infty} c_{\alpha,\ell}^{S,T} \frac{4\pi}{2\ell+1}\sum_{m=-\ell}^{\ell} Y_{\ell m}^*(\Omega_1) \\ &\quad \times \int d\Omega_2\, Y_{\ell m}(\Omega_2)|\Phi_0^{S,T}(\Omega_1,\Omega_2)|^2,\end{aligned} \tag{A9}$$

where we have used the addition theorem (A6) for $P_\ell(\cos\gamma)$.

In the *singlet* case (20), the Ω_2 integral equals $(\frac{1}{4\pi})^2\sqrt{4\pi}\delta_{\ell,0}\delta_{m,0}$ such that $\rho_\alpha^S(\Omega) = \frac{2}{4\pi}c_{\alpha,0}^S$. Normalization implies $c_{\alpha,0}^S = 1$ and, as expected, this surface density is uniform for all α,

$$\rho_\alpha^S(\Omega) = \frac{2}{4\pi} \quad (\text{all } \alpha \in \mathbb{R}). \tag{A10}$$

In the *triplet* case (21), the Ω_2 integral in Eq. (A9) is easily evaluated after expressing the products $Y_{1m}(\Omega_2)Y_{1m'}(\Omega_2)$ in terms of the functions $Y_{2m}(\Omega_2)$, with the result $\rho_\alpha^T(\Omega) = (c_{\alpha,0}^T - \frac{1}{5}c_{\alpha,2}^T)|Y_{00}|^2 + (c_{\alpha,0}^T - \frac{2}{3}c_{\alpha,1}^T + \frac{1}{5}c_{\alpha,2}^T)|Y_1(\Omega)|^2$. Consequently, normalization $\int d\Omega\, \rho_\alpha^T(\Omega) = 2$ yields the condition $c_{\alpha,0}^T = \frac{1}{3}c_{\alpha,1}^T$ which can be used to eliminate $c_{\alpha,1}^T$,

$$\begin{aligned}\rho_\alpha^T(\Omega) &= \frac{\tilde{c}_\alpha}{4\pi} + (2-\tilde{c}_\alpha)|Y_1(\Omega)|^2, \\ \tilde{c}_\alpha &\equiv c_{\alpha,0}^T - \frac{c_{\alpha,2}^T}{5}.\end{aligned} \tag{A11}$$

As it turns out, $\tilde{c}_\alpha \neq 2$ for all α except for one particular value $\alpha \approx -5.3$. Consequently, the triplet density is typically nonuniform. In particular, it is *not* the same for different values of α. Therefore, unfortunately, the triplet states $\Psi_\alpha^T(\Omega_1,\Omega_2)$ do not represent the state $\Psi_\alpha[\rho]$ in Eq. (1) for the triplet system.

APPENDIX B: STRICTLY CORRELATED ELECTRONS ($\alpha \to +\infty$)

In the strong-repulsion limit $\alpha \to \infty$ which is not accessible by perturbation theory, the two electrons are strictly correlated [8], staying always exactly at opposite positions on the sphere,

$$\lim_{\alpha\to\infty}|\Psi_\alpha(\Omega_1,\Omega_2;\sigma_1,\sigma_2)|^2 = \frac{\delta(\theta_1+\theta_2-\pi)\delta(\phi_1-\phi_2+\pi)}{4\pi\sin\theta_2}. \tag{B1}$$

At large but finite $\alpha \gg 1$, this strictly-correlated motion is superimposed by quantum-mechanical zero-point oscillations [8]. Driven by the strong repulsion $\alpha\hat{V}_{ee}$ between the electrons, these oscillations are fast. Therefore, we can study small oscillations around a frozen pair $\{(\theta_1^{(0)},\phi_1^{(0)}),(\theta_2^{(0)},\phi_2^{(0)})\}$ of strictly-correlated positions, for example $\{(\frac{\pi}{2},0),(\frac{\pi}{2},\pi)\}$. Writing

$$\begin{aligned}\theta_1 &= \frac{\pi}{2} + \delta\theta_1, \quad \phi_1 = \delta\phi_1, \\ \theta_2 &= \frac{\pi}{2} - \delta\theta_2, \quad \phi_2 = \pi + \delta\phi_2,\end{aligned} \tag{B2}$$

we introduce approximate Cartesian coordinates on the sphere with radius R ($\delta\theta_i, \delta\phi_i \ll 1$),

$$x_i = R\delta\phi_i, \quad y_i = R\delta\theta_i. \tag{B3}$$

Then the Hamiltonian (17) becomes

$$\hat{H}_\alpha[R] \approx \frac{m_e}{2}(\dot{x}_1^2+\dot{y}_1^2) + \frac{m_e}{2}(\dot{x}_2^2+\dot{y}_2^2) + \alpha V(\gamma). \tag{B4}$$

Writing $\delta\theta_1 - \delta\theta_2 \equiv \delta\theta$ and $\delta\phi_1 - \delta\phi_2 \equiv \delta\phi$, the interaction potential (16) can be expanded,

$$V_{ee}(\gamma) \approx \frac{e^2}{2R}\frac{1}{\sqrt{1-\frac{1}{4}(\delta\phi^2+\delta\theta^2)}} \approx \frac{e^2}{2R}\left[1+\frac{1}{8}(\delta\phi^2+\delta\theta^2)\right]. \tag{B5}$$

In terms of center-of-mass and relative coordinates, $X = \frac{1}{2}(x_1+x_2)$, $Y = \frac{1}{2}(y_1+y_2)$, $x = x_1 - x_2$, and $y = y_1 - y_2$, the Hamiltonian (B4) is separated into a free particle and an oscillator,

$$\begin{aligned}\hat{H}_\alpha[R] \approx{}& \frac{M}{2}(\dot{X}^2+\dot{Y}^2) + \frac{\mu}{2}(\dot{x}^2+\dot{y}^2) \\ &+ \alpha\left[\frac{e^2}{2R} + \frac{e^2}{16R^3}(x^2+y^2)\right].\end{aligned} \tag{B6}$$

In the ground state, the free particle (mass $M = 2m_e$) has only

potential energy $\alpha/2R$, while the oscillator (mass $\mu=\frac{m_e}{2}$) has the 2D zero-point energy $\frac{2}{2}\hbar\omega_\alpha=\hbar\sqrt{\alpha e^2/8\mu R^3}$,

$$E_\alpha^{S,T}[R]\approx\frac{\alpha e^2}{2R}+\frac{2}{2}\hbar\omega_\alpha=\frac{e^2}{2R}[\alpha+\sqrt{\alpha a_B/R}+O(\alpha^0)]. \tag{B7}$$

For $R=a_B$, this result is equivalent to the asymptotic expression for $\mathcal{E}_\alpha^{S,T}$ in Eq. (30).

APPENDIX C: STRONG-ATTRACTION LIMIT ($\alpha\to-\infty$)

In the strong-attraction limit $\alpha\ll-1$ the electron pair on the sphere forms a bound state in a 2D, asymptotically planar environment. We therefore consider two attractive electrons on a plane or, equivalently, a 2D positronium atom. For the wave function $\Psi(\mathbf{r}_1,\mathbf{r}_2;\sigma_1,\sigma_2)=U(\mathbf{r}_1,\mathbf{r}_2)\chi(\sigma_1,\sigma_2)$ (where $\mathbf{r}_1$ and $\mathbf{r}_2$ are 2D position vectors and σ_1, σ_2 are spin variables) we introduce center-of-mass and relative coordinates, $\mathbf{R}=\frac{1}{2}(\mathbf{r}_1+\mathbf{r}_2)$ and $\mathbf{r}=\mathbf{r}_1-\mathbf{r}_2$, respectively,

$$U(\mathbf{r}_1,\mathbf{r}_2)=u(\mathbf{r})e^{i\mathbf{K}\cdot\mathbf{R}}. \tag{C1}$$

In polar coordinates (r,φ), the Schrödinger equation for the relative wave function $u\mathbf{r}$) reads

$$-\frac{\hbar^2}{2\mu}\left[\frac{1}{r}\frac{\partial}{\partial r}\left(r\frac{\partial u(\mathbf{r})}{\partial r}\right)+\frac{1}{r^2}\frac{\partial^2 u(\mathbf{r})}{\partial\varphi^2}\right]-|\alpha|\frac{e^2}{r}u(\mathbf{r})=Eu(\mathbf{r})\times\left(\mu=\frac{m_e}{2}\right). \tag{C2}$$

The ansatz $u(\mathbf{r})=R(r)e^{im\varphi}$, with $R(r)=g(r)e^{-\epsilon r}$ and $\epsilon^2\equiv m_e|E|/\hbar^2$, yields the equation

$$g''(r)+\left(\frac{1}{r}-2\epsilon\right)g'(r)+\left(\frac{|\alpha|}{a_B r}-\frac{\epsilon}{r}-\frac{m^2}{r^2}\right)g(r)=0\quad(m=0,\pm1,\pm2,\dots). \tag{C3}$$

Inserting the expansion $g(r)=r^k\Sigma_{\nu=0}^{\infty}a_\nu r^\nu=\Sigma_{\nu=0}^{\infty}a_\nu r^{\nu+k}$, $a_0\neq0$, we obtain

$$r^{k-2}[a_0(k^2-m^2)]+\sum_{\nu=1}^{\infty}r^{k-2+\nu}\left\{a_\nu[(k+\nu)^2-m^2]+a_{\nu-1}\left[-2\epsilon\left(k+\nu-\tfrac{1}{2}\right)+\frac{|\alpha|}{a_B}\right]\right\}=0. \tag{C4}$$

This can be fulfilled only with $k^2=m^2$. Since $u(\mathbf{r})$ is regular at $r=0$, the correct choice is $k=|m|$. For the coefficients, we obtain the recursion relation

$$a_\nu=\frac{2\epsilon\left(|m|+\nu-\frac{1}{2}\right)-\frac{|\alpha|}{a_B}}{\nu^2+2|m|\nu}a_{\nu-1}\quad(\nu=1,2,3,\dots). \tag{C5}$$

Since $a_\nu/a_{\nu-1}\to2\epsilon/\nu$ as $\nu\to\infty$, the series must be finite [and $g(r)$ a polynomial] to avoid the divergence $g(r)\to e^{+2\epsilon r}$ as $r\to\infty$. Consequently, ϵ is restricted to the values

$$\epsilon_n=\frac{|\alpha|}{2a_B}\frac{1}{n+\frac{1}{2}}\quad(n\equiv|m|+\nu-1,\nu=1,2,3,\dots). \tag{C6}$$

The corresponding energy eigenvalues are

$$E_n=-\frac{\hbar^2\epsilon_n^2}{m_e}=-\frac{\alpha^2}{(2n+1)^2}\frac{e^2}{a_B}\quad(n=0,1,2,3,\dots). \tag{C7}$$

For $n=0,1$, these are (in atomic units) identical with the asymptotic energies (32) and (33). The corresponding eigenfunctions $u_{nm}^\alpha(r,\varphi)$ are

$$u_{00}^\alpha(r)=\frac{2|\alpha|}{\sqrt{2\pi}a_B}e^{-|\alpha|r/a_B},$$

$$u_{1m}^\alpha(r,\varphi)=\frac{2\alpha^2}{9\sqrt{3\pi}a_B^2}re^{-|\alpha|r/3a_B}e^{im\varphi}\quad(m=0,\pm1). \tag{C8}$$

Using the asymptotic correlation factors (32) and (33), respectively, these wave functions can also be extracted from the ansatz (24).

[1] R. G. Parr and W. Yang, *Density-Functional Theory of Atoms and Molecules* (Oxford University Press, New York, 1989); R. M. Dreizler and E. K. U. Gross, *Density Functional Theory* (Springer, Berlin, 1990).

[2] D. C. Langreth and J. P. Perdew, Solid State Commun. **17**, 1425 (1975); O. Gunnarsson and B. I. Lundqvist, Phys. Rev. B **13**, 4274 (1976).

[3] F. Colonna and A. Savin, J. Chem. Phys. **110**, 2828 (1999); R. Pollet, F. Colonna, T. Leininger, H. Stoll, H.-J. Werner, and A. Savin, Int. J. Quantum Chem. **91**, 84 (2003); A. Savin, F. Colonna, and R. Pollet, *ibid.* **94**, 166 (2003).

[4] A. Görling and M. Levy, Phys. Rev. B **47**, 013105 (1993); Phys. Rev. A **52**, 4493 (1995).

[5] M. Seidl, J. P. Perdew, and S. Kurth, Phys. Rev. Lett. **84**, 5070 (2000).

[6] J. Olsen, O. Christiansen, H. Koch, and P. Jørgensen, J. Chem. Phys. **105**, 5082 (1996).

[7] M. Seidl, J. P. Perdew, and M. Levy, Phys. Rev. A **59**, 51 (1999).

[8] M. Seidl, Phys. Rev. A **60**, 4387 (1999).

[9] M. Seidl, P. Gori-Giorgi, and A. Savin, Phys. Rev. A **75**, 042511 (2007).

[10] M. Seidl, J. P. Perdew, and S. Kurth, Phys. Rev. A **62**, 012502 (2000); **72**, 029904(E) (2005).

[11] M. Seidl, Phys. Rev. B **70**, 073101 (2004).

[12] C. Attaccalite, S. Moroni, P. Gori-Giorgi, and G. B. Bachelet, Phys. Rev. Lett. **88**, 256601 (2002).

[13] C. Møller and M. S. Plesset, Phys. Rev. **46**, 618 (1934).

[14] M. Seidl (unpublished).